Suitable location prediction for solar farms using Artificial Neural Networks

Jens Houbregs
Department of Science
UHasselt
Hasselt Univeristy
Hasselt, Belgium
jens.houbregs@student.uhasselt.be

Pietro Benecchi
Department of electronics, computer science and bioengineering
Polytechnic of Milan
Milan, Italy
pietro.benecchi@mail.polimi.it

Mirko Calvi
Department of electronics, computer science and bioengineering
Polytechnic of Milan
Milan, Italy
mirko.calvi@mail.polimi.it

Abstract

Optimal solar panels installation is complex. Traditional analysis is inefficient; current automated tools often lack broad accuracy or scalability. This projects explores neural networks for scalable solar farm site prediction. We have used CNNs to classify land cover and LSTM to forecast land costs. With this project, we aim to improve solar planning, facilitate increased utilization of renewable energy sources, and demonstrate the significant potential of AI in optimizing spatial resource allocation.

I. Introduction

The global imperative to transition towards sustainable energy systems has positioned solar power as a cornerstone of renewable energy strategies as can be seen in [6]. The efficacy of solar energy generation is, however, intrinsically linked to the optimal siting of photovoltaic installations. Selecting suitable locations for solar farms is a complex challenge, contingent upon a confluence of geographical, environmental, and infrastructural factors including terrain suitability, solar irradiance levels and land usage. Traditional methodologies for site selection often rely on manual terrain analysis using software such as Q-Gis and Arch-Gis, a process that is not only labor-intensive and time-consuming but also susceptible to inconsistencies, particularly when assessing large or remote geographical areas. While automated models have emerged, many are either geographically constrained in their application or have yet to achieve the desired levels of predictive accuracy necessary for robust, large-scale deployment such as [3].

This research explores the application of neural network architectures to advance the accuracy and computational efficiency of predictive models for solar farm site suitability. The primary objective is to ascertain whether a neural network-based methodology, utilizing a diverse range of geospatial datasets, can yield a more precise and scalable alternative to traditional assessment techniques and existing computational frameworks. We propose a multi-faceted approach involving the development of distinct neural network models to address specific predictive tasks. Initially, a Convolutional Neural Network (CNN) will be employed for semantic segmentation of land cover, with its outputs subsequently integrated with heatmap visualizations for spatial analysis. Furthermore, a time series analysis will be conducted to forecast future land costs, thereby providing stakeholders with critical data to evaluate the long-term investment viability. The training of these models will leverage a comprehensive dataset encompassing multispectral satellite imagery, Digital Elevation Models (DEMs) for topographical analysis, meteorological records, and data of existing solar installations.

By integrating these diverse data streams and employing a sophisticated deep learning methodology, this research aims to contribute a more refined and reliable tool for strategic solar energy planning, thereby supporting the accelerated adoption of renewable energy technologies. The findings are expected to demonstrate the utility of neural networks in addressing complex spatial decision-making problems within the renewable energy sector.

II. Related Works

The challenge of identifying optimal locations for solar energy infrastructure is increasingly being addressed with advanced computational techniques, moving beyond traditional site assessment methods. Neural networks, in particular, offer powerful tools for analyzing complex geospatial and temporal data pertinent to solar farm siting.

Several research efforts highlight the capabilities of deep learning in this domain. For instance, Sachit et al. (2022) [3]demonstrate a broader application of AI by developing a global spatial suitability map for solar and wind systems using machine learning models like Random Forest and Explainable AI (XAI). Their work underscores the utility of AI in integrating diverse geo-technical and environmental factors for large-scale suitability assessment, offering a complementary perspective to more focused neural network approaches by showcasing how model interpretability can inform strategic energy planning. This aligns with the goal of comprehensive site evaluation, even if the specific AI techniques differ from the deep learning focus of your project.

Also, the work by Mokarram et al. (2023) [4] is relevant as it showcases the use of Long Short-Term Memory (LSTM) networks for predicting solar power plant energy generation based on climate conditions, integrated with GIS for spatial analysis. While their study predicts energy output rather than land costs, it demonstrates the methodological applicability of LSTMs for time-series forecasting in the solar energy sector. This supports the premise of using similar recurrent neural network architectures, as proposed in our work, for predictive tasks such as forecasting future land costs, which is a critical economic variable in determining solar farm viability.

Furthermore, the direct identification and mapping of solar infrastructure using deep learning and satellite imagery is a rapidly advancing area. Robinson et al. (2025) [5] contribute significantly by presenting the "Global Renewables Watch," a global temporal dataset of solar photovoltaic farms derived from high-resolution satellite imagery using deep learning-based segmentation models. Their approach not only maps existing installations but also estimates construction dates and preceding land use types. This is highly pertinent to your project's aim of using Convolutional Neural Networks (CNNs) for semantic segmentation of land cover to identify suitable areas. It highlights the power of deep learning in processing vast amounts of satellite data for accurate, large-scale land use classification and infrastructure mapping, which are foundational steps in strategic solar farm siting.

These studies collectively illustrate the growing trend and success of employing sophisticated AI and neural network techniques to address various facets of solar energy planning, from broad suitability mapping and specific component prediction to the detailed identification of land characteristics and existing infrastructure from remote sensing data.

III. Dataset

The empirical validation of the proposed neural network models was conducted using a selection of publicly accessible datasets. A detailed description of each dataset is provided below.

1. *Semantic segmentation*

The primary dataset utilized was sourced from the DeepGlobe Land Cover Classification Challenge [2]. This benchmark dataset facilitates a multi-class image segmentation problem, specifically targeting the identification and delineation of seven distinct land cover categories: urban, agricultural, rangeland, forest, water, barren, and unknown. This dataset was mainly used for the training and validation of the first neural network.

2. *OpenTopography*

OpenTopography is a web-based data facility that provides open access to high-resolution topographic data and processing tools. It serves as a valuable resource for Earth science research, enabling the analysis of Earth surface features and processes. We have used this data source to collect topographic information about the terrain we are analyzing. OpenTopography gives you a .tif file containing but to interpret the data contained in the file we have use an open source library called xDEM. xDEM is tailored to perform quantitative analysis that implicitly understands the intricacies of elevation data, both from a georeferencing viewpoint (vertical referencing, nodata values, projection, pixel interpretation) and a statistical viewpoint (outlier robustness, specificities of 3D alignment and error structure).It exposes an intuitive object-based API to foster accessibility, and strives to be computationally scalable through Dask. We have used xDEM to retrieve the slope of a terrain (degrees) and the elevation values.

3. *Agricultural Land Prices*

The "Agricultural Land Prices by Region – Historical Data (until 2009)" dataset, by Eurostat, offers a comprehensive overview of agricultural land price trends across various European Union regions. This dataset encompasses annual data on the purchase prices of agricultural land, measured in euros per hectare. It includes detailed information on different land types, such as arable land and irrigable arable land, facilitating nuanced analyses of land value dynamics. By providing granular data at the regional level, the dataset supports comparative studies and contributes to a deeper understanding of the factors influencing land price fluctuations over time.

A. *Data Preprocessing*

1. *Segmentation analysis*

For the segmentation analysis, we initially preprocessed all the masks provided in the dataset. The dataset categorizes each mask into five primary land cover classes: Urban Land, Agricultural Land, Rangeland, Forest Land, Water, Barren Land, and Unknown.

To tailor the segmentation to our specific classification task, we redefined the mask categories by grouping Agricultural Land, Rangeland, and Barren Land as suitable areas for solar panel installation. The remaining categories—Urban Land, Forest Land, Water, and Unknown—were classified as not suitable for this purpose.

2. Agricultural land prices by region

Country	Avg. (€/ha)	Null (%)	Mean €/ha
Belgium	18632.20	52.0	18632.20
Czechia	1730.91	60.0	1730.91
Denmark	11963.84	0.0	11963.84
Germany	9921.01	40.0	9921.01
Ireland	8226.31	16.0	8226.31
Spain	6779.92	0.0	6779.92
France	4775.71	72.0	4775.71
Italy	12317.62	32.0	12317.62
Latvia	1818.62	68.0	1818.62
Lithuania	602.64	60.0	602.64
Luxembourg	16818.00	72.0	16818.00
Malta	129963.71	80.0	129963.71
Netherlands	32819.38	44.0	32819.38
Romania	389.48	76.0	389.48
Slovakia	1010.36	60.0	1010.36
Finland	4676.78	0.0	4676.78
Sweden	2264.94	28.0	2264.94
UK	11685.48	48.0	11685.48
England	8039.66	16.0	8039.66
Wales	6113.79	16.0	6113.79
Scotland	2919.10	28.0	2919.10
NIR (UK)	10800.41	16.0	10800.41

Table I: The table above shows the composition of the data for each country, some of which have already been removed due to the null% being zero.

After the longest sequence for each country, these are split in sequences of three and the target value. From this, the dataset is split into two sets, with two-thirds going towards the train dataset and one-third going towards the test dataset.

IV. Methods

This section is organized into distinct subdivisions, each detailing a specific component of the project.

1. Semantic segmentation

The first architecture is a **U-Net model** structured with an encoder-decoder paradigm. The encoder component utilizes a **ResNet50 network** [7], pretrained on the extensive ImageNet dataset. We have used an inductive transfer learning approach that allows the model to inherit powerful feature extraction capabilities. The pretrained ResNet50 backbone processes input images to generate rich feature maps. The decoder component then symmetrically upsamples these features to reconstruct a full-resolution segmentation map. This upsampling process is facilitated by transposed convolutions, and each stage incorporates batch normalization for training stability and ReLU activation functions to introduce nonlinearities. Also, skip connections are integrated, linking feature maps from the encoder directly to corresponding layers in the decoder. The final output layer maps the processed features to the required number of semantic classes. The complete architecture of a single decoder block is presented below. We have created five decoder blocks, followed by a final convolutional layer that projects the output into the classification task.

Decoder block architecture
Convolution Transpose 2D
ReLU
Convolution 2D
Batch Normalization
ReLU

We have also applied regularization techniques to prevent overfitting. In particular we have used **Reduce learning rate on Plateau** that adaptively lowers learning rates when validation metrics stall, aiding finer convergence. Ana Early Stopping that halts training if validation performance degrades, by saving the best model.

ResNet50 parameters	
Total Parameters	25,636,712
Trainable Parameters	25,583,592
Non-trainable Parameters	53,120

In our transfer learning approach, the ResNet50 parameters were initially frozen for the first 10 epochs to enable faster training. Subsequently, these parameters were unfrozen for the final 23 training epochs.

Instead the decoder part was always trainable during epochs.

Decoder parameters	
Total Parameters	24,494,881
Trainable Parameters	24,494,881
Non-trainable Parameters	0

2. Land price prediction

For handling time series data prediction we have used Long Short-Term Memory (LSTM) network to processes sequential data. We have created an LSTM layer with a embedded state of 128 and 2 layers, followed by a fully connected layer for output. This architecture is specifically employed for land usage calculations, learning temporal patterns to predict land use. Here is the full network architecture and trainable parameters:

Table II: **LSTM model Summary**

Layer	Output, Shape	Parameters
Generator		
LSTM	(1, 1, 128)	66,560
LSTM	(1, 128)	131,584
Dense	(1, 1)	129
Model Parameters		
Total Parameters		198,273
Trainable Parameters		198,273
Non-trainable Parameters		0

3. Suitable topography

After the prediction of suitable terrains for the installation of solar panels, we enhance the evaluation by considering the slope of the suitable terrain be overlapping the obtained mask with the mask of the terrain slope. A terrain is considered suitable if the slope under a threshold decided by the user. For our analysis, we have decided to use 20 degrees as default value in the function.

V. Evaluation

Figure I: Satellite input image

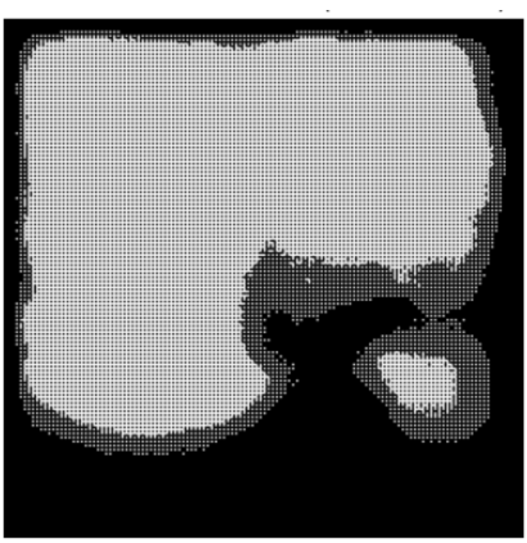

Figure II: suitable terrains mask

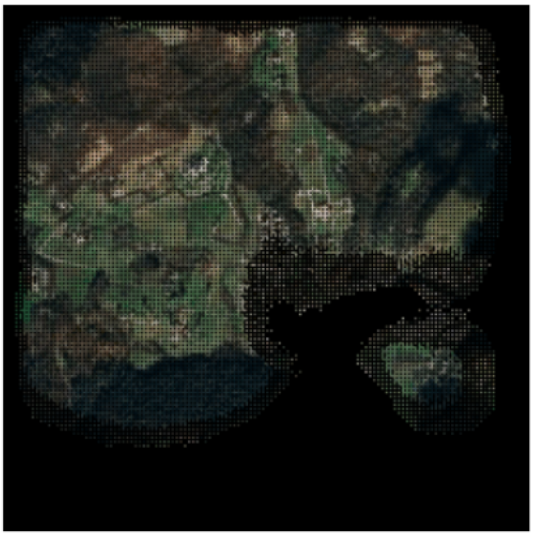

Figure III: suitable input terrains

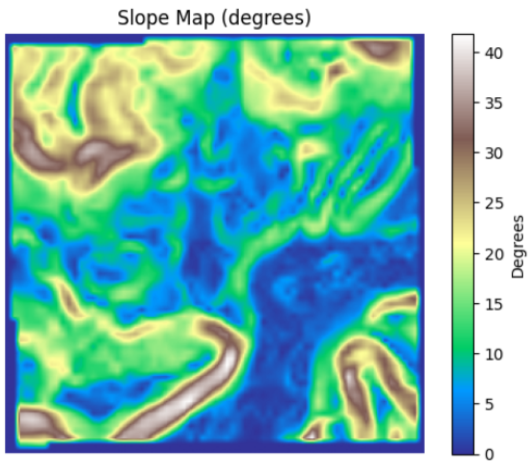

Figure IV: terrain slope

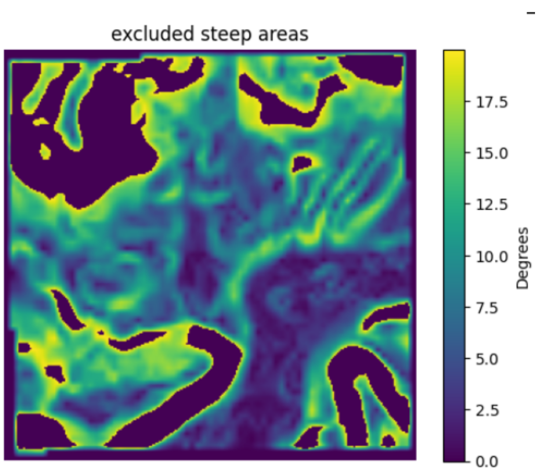

Figure V: terrain slope mask: threshold 20 degrees

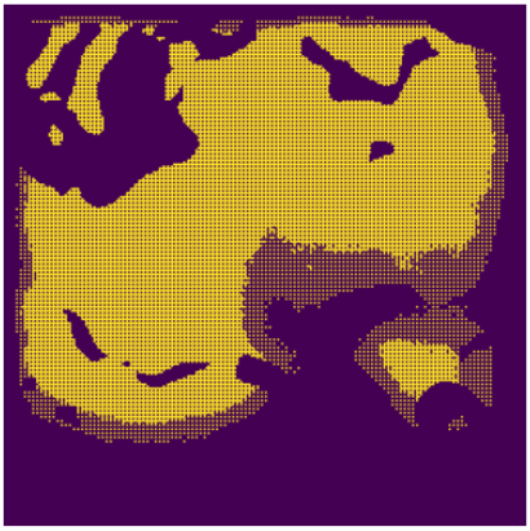

Figure VI: terrain slope mask and suitable terrains mask overlapped

1. Hardware

In this study, we utilized Google Colab with standard resources (free subscription) , using a T4 GPU.

A. Evaluation metrics

In this section, we provide definitions of the metrics that we used in evaluation part.

Confusion Matrix

A **confusion matrix** is a performance measurement tool for classification problems. It is a table that allows the evaluation of the performance of a classification algorithm by comparing the predicted labels with the actual labels. The matrix consists of four key elements:

- **True Positives (TP)**: The number of instances that were correctly predicted as positive.
- **False Positives (FP)**: The number of instances that were incorrectly predicted as positive.
- **True Negatives (TN)**: The number of instances that were correctly predicted as negative.
- **False Negatives (FN)**: The number of instances that were incorrectly predicted as negative.

The confusion matrix can be represented as:

	Predicted Positive	Predicted Negative
Actual Positive	TP	FN
Actual Negative	FP	TN

Recall and Accuracy

Two important metrics derived from the confusion matrix are **Recall** and **Accuracy**.

Recall (Sensitivity or True Positive Rate)

Recall measures the ability of a classifier to correctly identify positive instances. It is the ratio of correctly predicted positive observations to the total actual positives.

$$\text{Recall} = \frac{TP}{TP + FN}$$

A high recall indicates that most of the actual positive instances were correctly identified, but it may also imply that some negative instances were incorrectly classified as positive.

Accuracy

Accuracy measures the overall performance of the classifier by calculating the proportion of correctly classified instances (both positive and negative) to the total number of instances.

$$\text{Accuracy} = \frac{TP + TN}{TP + TN + FP + FN}$$

For semantic classification we have used Intersection over Union (IoU). It measures the overlap between two areas: the predicted bounding box and the ground truth bounding box.

The IoU is calculated as the area of the intersection between the predicted and ground truth boxes divided by the area of their union. A higher IoU means a better prediction.

$$\text{IoU} = \frac{A_{\text{intersection}}}{A_{\text{union}}}$$

1. Segmentation instances

The learning algorithm was configured to train the neural network for a maximum of 50 epochs. Early stopping, with a patience parameter set to 7 epochs, was implemented to prevent overfitting. Optimal model parameters were identified at epoch 33, achieving a validation loss of 0.2983. The Cross-Entropy Loss function was utilized as the training criterion,

$$L = -\frac{1}{n} \sum_{i=1}^{n} [y_i \log(\hat{y}_i) + (1 - y_i) \log(1 - \hat{y}_i)]$$

and optimization was performed using the Adam optimizer. The total training duration was approximately 1 hour and 28 minutes. We have also tested the network with a subset of DeepGloabl dataset and performed an confusion matrix analysis. The final results are:

Accuracy	0.8003
Precision	0.7309
Recall	0.8007
F1 score	0.8095
Specificity	0.7780
IoU	0.6843

2. Land prediction

We have trained the LSTM architecture for 2000 epochs reaching a training loss function of 0.3850. We have used the mean quadratic error as loss function

$$L = \frac{1}{2n} \sum_{i=1}^{n} (y_i - \hat{y}_i)^2$$

and Adam Optimizer for gradient descent. We have also performed an analysis with a test set reaching a loss of 0.2288.

B. Conclusion

We have proposed the application of neural networks as a solution for enhancing the precision and scalability of site suitability predictions. By leveraging diverse geospatial datasets and advanced machine learning models, the study intends to deliver a refined planning tool. Also, we have shown how AI can resolve complex geospatial problems within the energy sector.

VI. Future work

Future work of this project can be based on three main parts:

1. **Integrating Enhanced Tabular Data**

   The primary goal is to incorporate more granular land price data. We were not able to get comprehensive land valuation due to API cost. With proper founding, we can explore alternative data acquisition and fusion techniques. This will improve model accuracy and analysis of land value drivers.

2. **Expanding Geographically for Cross-Contextual Validation**

   Systematic expansion to diverse countries is critical for generalization. Applying models in new regions will test their robustness, identify universal versus context-specific aspects, and aid in context-aware models.

3. **Advancing Image-Based Feature Extraction**

   Improving direct extraction of geospatial features like land slope from imagery is key. We may use computer vision and deep learning to overcome current limitations in deriving slope and other feature. This will enhance our capabilities in out model predictions.

4. **Suitabilty Index**

   The initial concept for this project involved developing a Mixture of Experts (MoE) model to predict a suitability index based on satellite imagery, heatmaps, and tabular weather data. However, this approach was ultimately abandoned due to the unavailability of free APIs and the lack of reliable ground-truth parameters required for supervised learning. In the future, with adequate funding to access appropriate APIs and further research into relevant suitability indicators, this idea could be revisited and pursued more effectively.

VII. Usage of AI based tools

In the development of our study, AI-based tools like ChatGPT 3.5 and Gemini DeepResearch were incorporated and mainly utilized to refine the structure of this paper, enhance the readability, and improve the overall clarity of our research. These tools assisted us by organizing complex concepts into clear explanations, ensuring that technical concepts were effectively communicated. How-ever, while it provided valuable refinements, all technical con- tent, analyses, and conclusions were independently developed and reviewed to ensure accuracy and relevance. Overall, the integration contributed to a more polished presentation of our findings.

References

[1] Gharahbagh, A.A., Hajihashemi, V., Machado, J.J.M. and Tavares, J.M.R.S. (2025). Land Cover Classification Model Using Multispectral Satellite Images Based on a Deep Learning Synergistic Semantic Segmentation Network. Sensors, [online] 25(7), p.1988. doi:https://doi.org/10.3390/s25071988.

[2] Demir, I., Koperski, K., Lindenbaum, D., Pang, G., Huang, J., Basu, S., Hughes, F., Tuia, D. and Raskar, R. (2018). DeepGlobe 2018: A Challenge to Parse the Earth through Satellite Images. 2018 IEEE/CVF Conference on Computer Vision and Pattern Recognition Workshops (CVPRW), [online] pp.172–17209. doi:https://doi.org/10.1109/CVPRW.2018.00031.

[3] Mourtadha Sarhan Sachit, Mohd, Z., Ahmad Fikri Abdullah, Mohd, S. and Barakat, M. (2022). Global Spatial Suitability Mapping of Wind and Solar Systems Using an Explainable AI-Based Approach. ISPRS international journal of geo-information, 11(8), pp.422–422. doi:https://doi.org/10.3390/ijgi11080422.

[4] Mokarram, M., Aghaei, J., Mokarram, M.J., Mendes, G.P. and Mohammadi-Ivatloo, B. (2023). Geographic information system-based prediction of solar power plant production using deep neural networks. IET Renewable Power Generation, 17(10), pp.2663–2678. doi:https://doi.org/10.1049/rpg2.12781.

[5] Robinson, C., Ortiz, A., Kim, A., Dodhia, R., Zolli, A., Nagaraju, Shivaprakash K, Oakleaf, J., Kiesecker, J. and Lavista, J.M. (2025). Global Renewables Watch: A Temporal Dataset of Solar and Wind Energy Derived from Satellite Imagery. [online] arXiv.org. Available at: https://arxiv.org/abs/2503.14860 [Accessed 29 May 2025].

[6] IRENA (2018). GLOBAL ENERGY TRANSFORMATION About IRENA. [online] Available at: https://www.irena.org/-/media/Files/IRENA/Agency/Publication/2018/Apr/IRENA_Report_GET_2018.pdf.

[7] He, K., Zhang, X., Ren, S. and Sun, J. (2015). Deep Residual Learning for Image Recognition. [online] arXiv.org. Available at: https://arxiv.org/abs/1512.03385.